Proc. Natl. Acad. Sci. USA
Vol. 96, pp. 657–662, January 1999
Medical Sciences

Nitric oxide synthase in cardiac sarcoplasmic reticulum

KAI Y. XU*†, DAVID L. HUSO‡, TED M. DAWSON§, DAVID S. BREDT¶, AND LEWIS C. BECKER*†

*Department of Medicine, Division of Cardiology and ‡Division of Comparative Medicine, Johns Hopkins Medical Institutions, Baltimore, MD 21224; §Department of Neurology and Neuroscience, Johns Hopkins Medical Institutions, Baltimore, MD 21287; and ¶Department of Physiology, University of California School of Medicine, San Francisco, CA 94143

Edited by Solomon H. Snyder, Johns Hopkins University School of Medicine, Baltimore, MD, and approved November 6, 1998 (received for review July 1, 1998)

ABSTRACT **$NO^{\bullet}$ is a free radical that modulates heart function and metabolism. We report that a neuronal-type NO synthase (NOS) is located on cardiac sarcoplasmic reticulum (SR) membrane vesicles and that endogenous $NO^{\bullet}$ produced by SR-associated NOS inhibits SR Ca^{2+} uptake. Ca^{2+}-dependent biochemical conversion of L-arginine to L-citrulline was observed from isolated rabbit cardiac SR vesicles in the presence of NOS substrates and cofactors. Endogenous $NO^{\bullet}$ was generated from the vesicles and detected by electron paramagnetic resonance spin-trapping measurements. Immunoelectron microscopy demonstrated labeling of cardiac SR vesicles by using anti-neuronal NOS (nNOS), but not anti-endothelial NOS (eNOS) or anti-inducible NOS (iNOS) antibodies, whereas skeletal muscle SR vesicles had no nNOS immunoreactivity. The nNOS immunoreactivity also displayed a pattern consistent with SR localization in confocal micrographs of sections of human myocardium. Western blotting demonstrated that cardiac SR NOS is larger than brain NOS (160 vs. 155 kDa). No immunodetection was observed in cardiac SR vesicles from nNOS knockout mice or with an anti-nNOSμ antibody, suggesting the possibility of a new nNOS-type isoform. ^{45}Ca uptake by cardiac SR vesicles, catalyzed by Ca^{2+}-ATPase, was inhibited by $NO^{\bullet}$ produced endogenously from cardiac SR NOS, and 7-nitroindazole, a selective nNOS inhibitor, completely prevented this inhibition. These results suggest that a cardiac muscle nNOS isoform is located on SR of cardiac myocytes, where it may respond to intracellular Ca^{2+} concentration and modulate SR Ca^{2+} ion active transport in the heart.**

NO synthase (NOS) isoforms [neuronal NOS (nNOS), inducible NOS (iNOS), endothelial NOS (eNOS), and neuronal NOSμ (nNOSμ)], have been identified in cardiac and skeletal muscle (1–7). $NO^{\bullet}$, the product of NOS, has emerged as an important physiological regulator of calcium homeostasis (8) and myocardial contractile function (5) through interactions with both L-type calcium channels in cardiac myocytes (8) and the ryanodine receptor (RyR) (9). The sarcoplasmic reticulum (SR) in cardiomyocytes sequesters and releases graded levels of calcium ions near cytosolic contractile proteins to regulate contraction and relaxation of the heart. Although eNOS has been recently reported to copurify with the cardiac muscle RyR Ca^{2+} release channel (10), little is known about intracellular NOS sources or $NO^{\bullet}$ targets in cardiomyocytes and their roles in cardiac function. Here we report that cardiac muscle SR clearly expresses endogenous NOS activity and that endogenous $NO^{\bullet}$ can modify SR calcium uptake by inhibiting Ca^{2+}-ATPase. Furthermore, our data suggest that the predominant isoform present on the SR of cardiomyocytes is an nNOS isoform.

The publication costs of this article were defrayed in part by page charge payment. This article must therefore be hereby marked "*advertisement*" in accordance with 18 U.S.C. §1734 solely to indicate this fact.

PNAS is available online at www.pnas.org.

METHODS

Isolation of Cardiac SR Vesicles. Cardiac muscle SR vesicles were prepared from hearts of New Zealand White rabbits or from knockout and wild-type, C57BL6 mice (Charles River Breeding Laboratories) according to the method of Chu *et al.* (11) with modifications similar to those described previously (12). Animal care was in accordance with institutional guidelines. The final vesicles were resuspended in 10 mM Tris·HCl and 0.29 M sucrose buffer, pH 7.4, and stored at −70°C. Protein concentration was determined by the method of Lowry *et al.* (13).

Determination of NOS Activity. NOS activity was measured by monitoring the conversion of L-[^{3}H]arginine to L-[^{3}H]citrulline (14). For routine assays, 0.1 mg of vesicles and 10 μl of 100 nM L-[^{3}H]arginine were added to 40 μl of buffer containing 50 mM Tris (pH 7.4), 1 mM NADPH, 0.2 mM $CaCl_2$, 0.1 μM calmodulin (CaM), 2 μM flavin adenine dinucleotide (FAD), 2 μM flavin mononucleotide (FMN), and 3 μM of tetrahydrobiopterin (BH_4). After incubation for 30 min at 23°C, the reaction was stopped with 0.4 ml of 50 mM Hepes (pH 5.5) and 2 mM EGTA, and then applied to a 1-ml column of Dowex AG50WX-8 (Na^+), which was eluted with 2 ml of water. The L-[^{3}H]citrulline, being ionically neutral at pH 5.5, flowed through the column completely. The NOS activity was then quantitated by determining the radioactivity in the flow through.

Electron Paramagnetic Resonance (EPR) Measurements. Spin trapping measurements of $NO^{\bullet}$ radicals were performed in a flat cell at room temperature. The final concentrations of *N*-methyl-D-glucamine dithiocarbamate (MGD), Fe^{2+}, vesicles, Ca^{2+}, CaM, NADPH, FAD, FMN, BH_4, L-arginine, D-arginine, and superoxide dismutase (SOD) were 5 mM, 1 mM, 0.6 mg/ml, 0.2 mM, 0.1 μM, 1 mM, 2 μM, 2 μM, 3 μM, 2 mM, 2 mM, and 300 units/ml, respectively. The EPR spectra was recorded immediately after the spin trap solution was infused by using an IBM-Bruker ER 300 spectrometer operating at x-band with a transverse magnetic 110 cavity. The spectrometer settings were as follows: modulation frequency, 100 kHz; modulation amplitude, 1 G; scan time 1.0 min; microwave power, 80 mW; and microwave frequency, 9.7 GHz.

Western Blotting. The Opti-4CN Goat Anti-Mouse Detection Kit was used for the Western Blotting experiments (Bio-Rad). For purposes of nNOS immunodetection, three different antibodies were used. The anti-nNOSα antibody was raised against an N-terminal fusion protein encoded by exon 2 of nNOS and recognizes nNOSα (15). The anti-nNOS

This paper was submitted directly (Track II) to the *Proceedings* office.
Abbreviations: NOS, NO synthase; iNOS, inducible NOS; eNOS, endothelial NOS; nNOS, neuronal NOS; SR, sarcoplasmic reticulum; EPR, electron paramagnetic resonance; RyR, ryanodine receptor; CaM, calmodulin; BH_4, tetrahydrobiopterin; MGD, *N*-methyl-D-glucamine dithiocarbamate; SOD, superoxide dismutase; 7-NI, 7-nitroindazole; TRIM, 1-(2-trifluoromethylphenyl)imidazole; AMT, 2-amino-5,6-dihydro-6-methyl-4*H*-1,3-thiazine.
†To whom reprint requests should be addressed. e-mail: kxu@welchlink.welch.jhu.edu and lbecker@welchlink.welch.jhu.edu.

antibody was purchased form Affinity BioReagents (Golden, CO) and was raised against amino acids 724–739 of nNOS. The anti-nNOSμ antibody was raised against a peptide selective for nNOSμ as previously described (4).

Immunogold Labeling. Cardiac muscle SR vesicles (right side-out) were prepared from hearts of New Zealand White rabbits as described previously (12). Immunogold labeling (16) was performed by adsorbing SR vesicles (0.04 μg/ml) on copper grids and incubating the grids with the primary antibodies [anti-eNOS (PA1–037), anti-iNOS (PA1–036), and anti-nNOS (PA3–032) for the single labeling; anti-SERCA2 (MA3–910), anti-Na^+,K^+-ATPase (MA3–928), and anti-phospholamban (MA3–922) for the double labeling, (Affinity BioReagents)] diluted 1:250 in PBS. After 30 min of incubation at room temperature, the grids were washed with PBS and then incubated for 30 min with a secondary antibody (donkey anti-mouse IgG or anti-rabbit IgG from Jackson ImmnoResearch) conjugated to 12 nm of colloidal gold diluted 1:40 in PBS. After the labeling, all grids were contrasted with lead citrate and examined on a Zeiss 10A transmission electron microscope operating at 80 kV. Double immunogold labeling was performed by incubating grids with a second primary antibody (anti-nNOS) diluted 1:250 in PBS after the first molecule (Ca^{2+}-ATPase, Na^+,K^+-ATPase, or phospholamban) was labeled with primary and secondary antibodies. After a 30-min incubation, the grids were rinsed with PBS and then incubated for 30 min with a second secondary antibody conjugated to 12-nm colloidal gold diluted 1:40 in PBS. The grids were then washed, stained, dried, and viewed as described above.

Immunofluorescent Labeling. The labeling was performed as described with modifications (17). A biopsy of human ventricular muscle from an explanted heart was frozen in liquid nitrogen-cooled isopentane, embedded in OCT, and stored at -80°C until sectioned at 6 μm. The sections were dried onto glass slides, rehydrated, and blocked with PBS 10% horse serum. Primary mAbs to cardiac SR Ca^{2+}-ATPase (SERCA2, Affinity BioReagents), RyR (MA3–925, Affinity BioReagents), Na^+,K^+-ATPase (Affinity BioReagents), nNOS (N31020, Transduction Laboratories, Lexington, KY) and simian immunodeficiency virus Gag (Karen Kent, AIDS Research and Reference Reagents) were used at 1:100. Donkey anti-mouse antibodies labeled with Cy3 (Jackson Immuno Research) were used at 1:500 as secondary antibodies. All antibodies were diluted in PBS 10% horse serum. Immunofluorescent images of each section were captured during confocal laser microscopy by using a Zeiss LSM 410 system.

^{45}Ca Uptake. Cardiac SR vesicles were incubated with or without substrates specific for nNOS in the presence and absence of 7-nitroindazole (7-NI). The reaction mixture contained 0.6 mg/ml vesicles, ^{45}Ca (1 μCi/ml), Ca^{2+} (0.2 mM), P^1,P^5-di(adenosine-5′)pentaphosphate (0.4 mM), oligomycin (4 μg/ml), ruthenium red (30 nM), and Mg^{2+} (4 mM) (12). The final concentrations of NOS substrates and cofactors were the same as described for the EPR measurements. ^{45}Ca uptake was initiated by the addition of MgATP (2 mM) to the reaction mixture for 30 min at 37°C or for 60 min (30 min at 23°C and 30 min at 37°C). The reaction was stopped by pelleting the samples at 14,000 rpm for 10 min, and the pellet was washed and dissolved in 0.5 ml of 10% SDS solution. An aliquot was taken from each sample, and the radioactivity was determined by a β-scintillation counter. The results were expressed as thapsigargin-sensitive ^{45}Ca uptake. Three hundred units per milliliter SOD were present in all experimental samples to ensure the specificity of the inhibition. EPR spin-trapping measurements also indicated that NO$^\bullet$ was the only detectable free radical present in these reaction mixtures (data not shown).

RESULTS

All of the NOS isoforms catalyze a 5-electron oxidation of an amidine nitrogen of L-arginine to generate L-citrulline and NO$^\bullet$. During the biochemical analysis of isolated rabbit cardiac SR vesicles, we observed endogenous NOS activity, as measured by the conversion of L-[^{3}H]arginine (100 nM) to L-[^{3}H]citrulline in the presence of cofactors [Ca^{2+} (0.2 mM), CaM (0.1 μM), NADPH (1 mM), FAD (2 μM), FMN (2 μM), and BH_4 (3 μM)] (Fig. 1*a*, lane A). NOS activity was not present in controls containing substrates alone without vesicles (Fig. 1*a*, lane B) or if vesicles were first boiled before addition of substrates (Fig. 1*a*, lane C). Cardiac SR NOS activity was

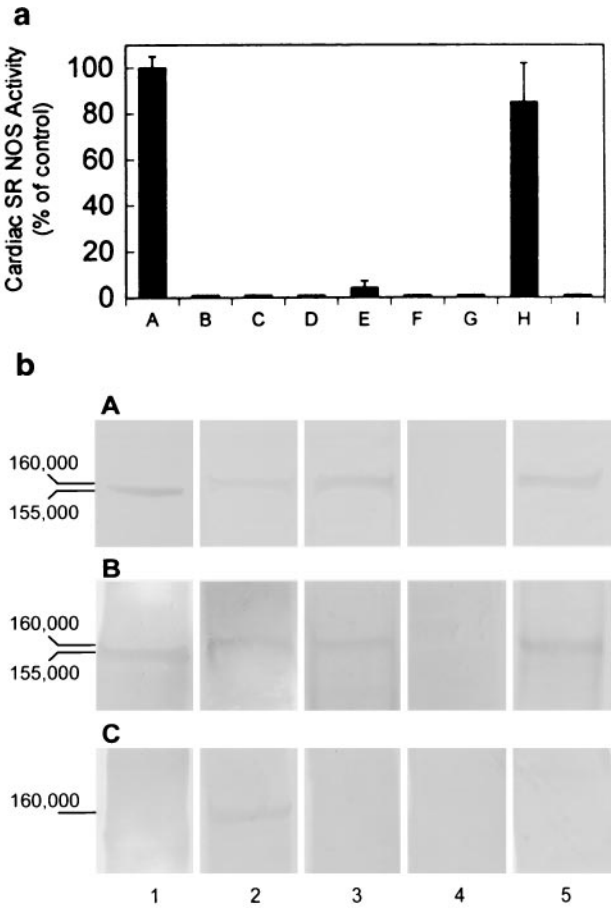

FIG. 1. (*a*) NO synthase activity was found in isolated cardiac SR vesicles. Lane A: control, in the presence of NOS substrates and cofactors: Ca^{2+}, CaM, NADPH, FMN, FAD, [^{3}H]arginine, and BH_4; lane B: in the presence of NOS substrates without vesicles; lane C: boiled vesicles + NOS substrates and cofactors; lane D: in the absence of Ca^{2+}; lane E: with EGTA and NOS substrates and cofactors; lane F: with 10 μM 7-NI; lane G: with 60 μM TRIM; lane H: with 10 nM AMT; and lane I: iNOS in the presence of 10 nM AMT. These results demonstrate that SR NOS activity is Ca^{2+} dependent and is sensitive to nNOS selective inhibitors, indicating the existence of NOS in cardiac SR vesicles and the specificity of a neuronal-type NOS enzymatic activity. The data represent a mean of six independent experiments. (*b*) Western blot analysis of cardiac SR NOS. Cardiac SR vesicles were fractionated by electrophoresis through a 7.5% SDS-polyacrylamide gel and transferred to nitrocellulose. Incubated with Affinity BioReagents anti-nNOS antibody (*bA*), with anti-nNOSα antibody (*bB*), and with anti-nNOSμ antibody (*bC*). Column 1: rat brain homogenate; 2: mice heart homogenate; 3: mice cardiac SR vesicles; 4: nNOS knockout mice cardiac SR vesicles; and 5: rabbit cardiac SR vesicles. All of the samples were 30 μg (total protein) per lane. Both rabbit and mice cardiac SR NOS were detected by anti-nNOS and anti-αnNOS antibodies. The results also show that the denatured molecular masses of rat brain NOS and cardiac SR NOS were $\approx$155 and 160 kDa, respectively.

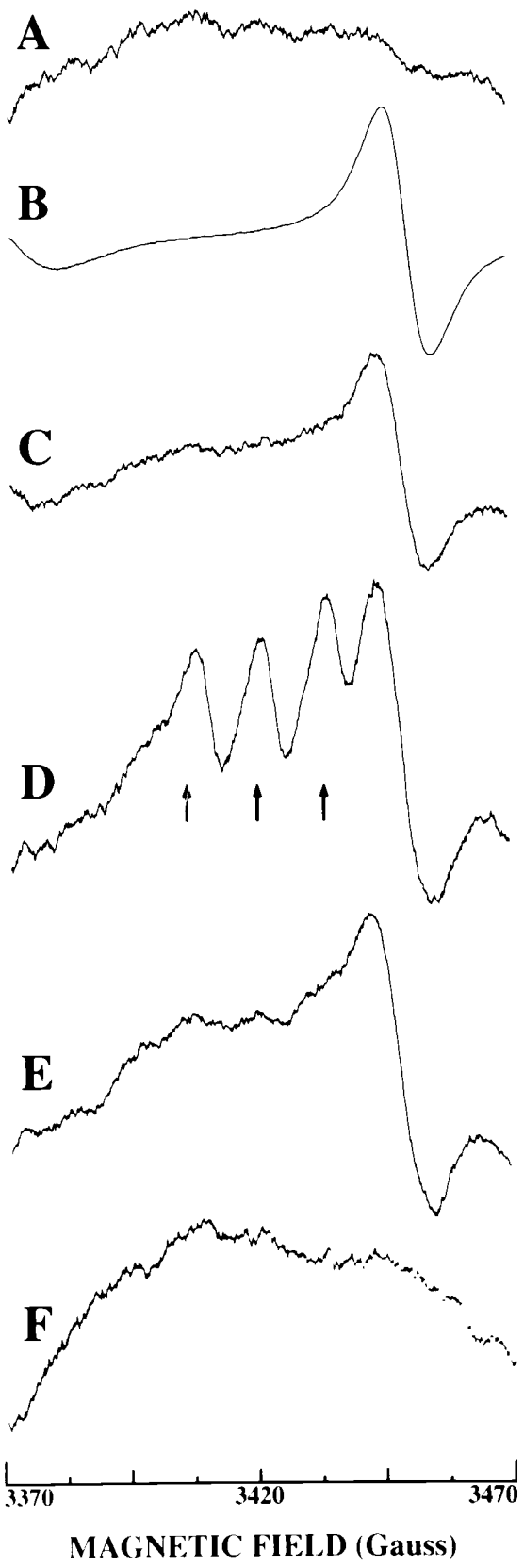

FIG. 2. EPR spectra of NO• formation from cardiac SR vesicles in the presence of a $Fe(MGD)_2$ complex under various conditions for 60 min at room temperature. $Fe(MGD)_2$ only (*A*); + SOD in condition *A* (*B*); + a mixture of NOS substrates and cofactors in condition *B* (*C*); + cardiac vesicles in condition *C* (*D*); + 7-NI in condition *D* (*E*); and + D-arginine in the presence of vesicles and cofactors (*F*) (see *Methods* for the final concentrations of the reaction components).

abolished when EGTA (2 mM) was added (Fig. 1*a*, lane E) and no NOS activity was seen in the absence of Ca^{2+} (Fig. 1*a*, lane D), demonstrating that cardiac SR NOS activity is Ca^{2+} dependent. It has been reported that 7-NI and 1-(2-trifluoromethylphenyl)imidazole (TRIM) are potent, selective inhibitors of nNOS (18, 19), with an IC_{50} for 7-NI of 0.71 μM for rat nNOS and of 28.2 μM for TRIM for mouse nNOS (20). TRIM is a poor inhibitor of bovine aortic endothelial NOS with an IC_{50} of 1057.5 μM (20). The complete inactivation of cardiac SR NOS activity under our experimental conditions required 10 μM 7-NI (Fig. 1*a*, lane F) or 60 μM TRIM (Fig. 1*a*, lane G). These results suggest that cardiac SR NOS is an nNOS-type NOS and is not eNOS. The potent iNOS inhibitor, 2-amino-5,6-dihydro-6-methyl-4*H*-1,3-thiazine (AMT, 10 nM), completely inhibited iNOS (Fig. 1*a*, lane I), but only 15% inhibition of cardiac SR NOS was seen at the same concentration (Fig. 1*a*, lane H), indicating that cardiac SR NOS is not iNOS.

It has been reported that both skeletal and cardiac muscle express nNOSμ isoform (4). To evaluate whether cardiac SR NOS is nNOSμ protein, Western blot experiments were performed by using an anti-nNOSμ antibody. nNOSμ was detected in whole heart homogenates. Cardiac SR NOS also was detected by anti-nNOS and anti-nNOSα antibodies in both isolated rabbit and mouse cardiac SR vesicles, but not in the nNOS knockout mouse cardiac SR vesicles (Fig. 1*b*). In contrast, no detection occurred when the same vesicles were incubated with anti-nNOSμ antibody, suggesting that cardiac SR NOS is not an nNOSμ isoform. The results also show that cardiac SR NOS was larger than brain NOS (160 vs. 155 kDa). Taken together, these results suggest the possibility of a potential nNOS isoform associated with the cardiac SR membrane.

We next examined whether NO• is produced by cardiac SR vesicles by using the NO•-specific spin trap Fe^{2+} complex, $Fe(MGD)_2$ (21). EPR spectroscopy is a technique capable of directly measuring molecules with unpaired electron spin such as NO•. The EPR spin-trapping measurements confirmed that NO• was generated endogenously from isolated SR vesicles in the presence of NOS substrates and cofactors (Fig. 2*D*, a triplet spectrum). This endogenous NO• production was inhibited by the nNOS selective inhibitor, 7-NI (Fig. 2*E*) and could not be supported by D-arginine (Fig. 2*F*). The results further demonstrate functional NOS in cardiac SR vesicles. To ensure the specificity of endogenous NO• generation, SOD was present in all of the reaction samples, except Fig. 2 *A* and *B*, to prevent superoxide generation from BH_4 autoxidation (22) or any other source. NO• radicals were not detected in a mixture of SOD (300 units/ml), Ca^{2+} (0.2 mM), L-arginine (2 mM), NADPH (1 mM), FAD (1 μM), FMN (1 μM), CaM (0.1 μM), and BH_4 (3 μM) as shown in Fig. 2*C*. Moreover, neither the $Fe(MGD)_2$ spin-trapping reagent alone (Fig. 2*A*) nor with SOD (Fig. 2*B*) showed any detectable NO• radical signal.

Immunofluorescence localization of cardiac SR NOS was next performed in human ventricular myocardial sections to determine how its subcellular location compared with the restricted sarcolemmal membrane localization pattern that has been reported for skeletal muscle (1–4, 7). By using a mAb (Transduction Laboratories) specific to nNOS, the results revealed a combination of a longitudinal and transverse linear intracellular pattern in the heart muscle (Fig. 3*aA*) consistent with what has been described for antigens localized to the longitudinal and junctional SR (23, 24). For comparison, we stained sections with mAbs specific for the cardiac Ca^{2+}-

These results show that 7-NI sensitive, endogenous NO• (a triplet spectrum) is generated by the isolated cardiac SR vesicles. The data are presented from one of four similar independent experiments in each case.

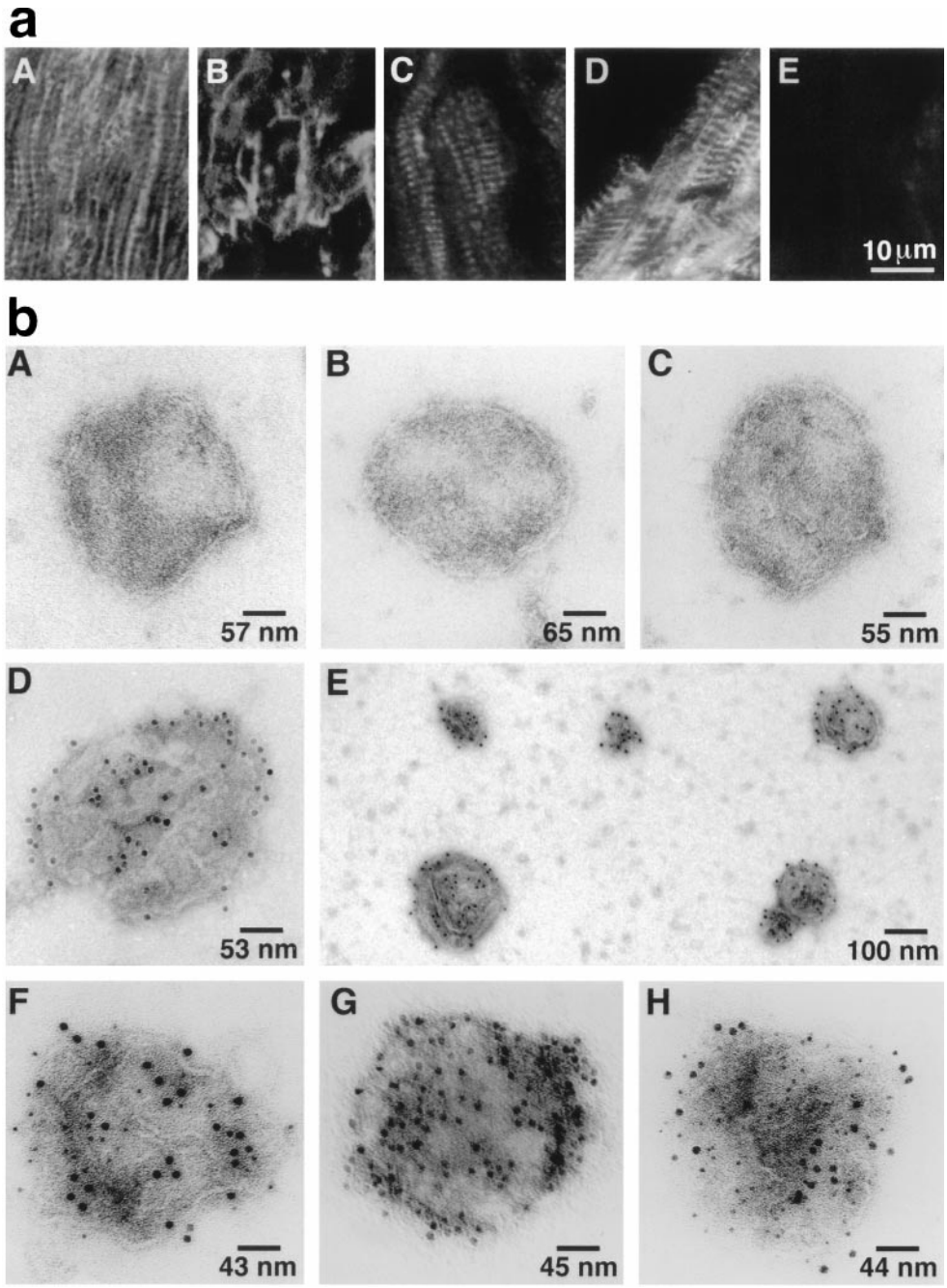

FIG. 3. (*a*) Immunofluorescent localization of cardiomyocyte antigens with mAbs on cryostat sections of human ventricular myocardium by laser-scanning confocal microscopy. (*aA*) nNOS indirect immunofluorescent labeling (IIL) shows a linear longitudinal and transverse, striated pattern of labeling; Na^+,K^+-ATPase IIL demonstrates a distinctly different sarcolemma pattern of labeling of the human heart section (*aB*); RyR IIL (*aC*) and SERCA2 IIL (*aD*) have a similar pattern of labeling as NOS IIL suggesting SR localization of NOS rather than exclusive sarcolemma localization in cardiac muscle; an irrelevant anti-viral protein mAb (*aE*) used at the same concentration as the other primary mAbs, has only low levels of background fluorescence. (*b*) Single immunogold labeling. SR vesicles were incubated with specific primary antibodies and a secondary antibody conjugated to 12 nm of colloidalgold. Control vesicles in the absence of primary antibody (*bA*); with anti-eNOS (*bB*); with anti-iNOS (*bC*); and single vesicle (*bD*) and a group of vesicles (*bE*) with anti-nNOS. Electron photomicrographs show that only nNOS is broadly dispersed on the surface of cardiac muscle SR membrane vesicles. Double immunogold labeling: Ca^{2+}-ATPase (6 nm gold particles) and nNOS (12 nm) (*bF*); Na^+, K^+-ATPase (6 nm) and nNOS (12 nm) (*bG*); and phospholamban (6 nm) and nNOS (12 nm) (*bH*). Each vesicle represents hundreds of similar labeled or unlabeled vesicles in each condition. The results show that cardiac SR Ca^{2+}-ATPase and phospholamban coexist with a SR neuronal-type NOS. Absence of Na^+,K^+-ATPase on the SR vesicles further demonstrates the vesicles represent SR rather than sarcolemma.

ATPase (SERCA2) and the RyR, both of which have previously been shown to be localized to the longitudinal and junctional SR (25, 26). The SR antigens, RyR (Fig. 3*aC*) and SERCA2 (Fig. 3*aD*), had a similar immunofluorescent pattern to nNOS (Fig. 3*aA*). In contrast, Na^+,K^+-ATPase, which is exclusively a sarcolemmal antigen, had a completely different pattern of immunofluorescent staining (Fig. 3*aB*). Control sections stained with a mAb to an irrelevant viral protein displayed only weak background fluorescence (Fig. 3*aE*).

To confirm the immunological identity and localization of the NOS isoform responsible for endogenous NOS activity in cardiac SR vesicles, immunogold labeling and electron microscopy were performed. Anti-nNOS immunoreactivity was broadly distributed on isolated cardiac SR membrane vesicles

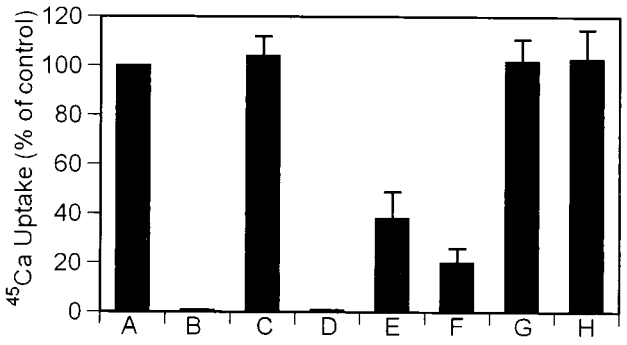

FIG. 4. Effect of endogenous NO• on cardiac SR ^{45}Ca uptake under various conditions. Vesicles in the absence of NOS substrates, cofactors, and SOD (*A*); −SOD + thapsigargin (*B*) (Tg, a specific inhibitor of Ca^{2+}-ATPase); vesicles + SOD (*C*); + SOD + Tg (*D*); condition *C* in the presence of NOS substrates and cofactors for 30 min (*E*), or for 60 min (*F*) (30 min at 23°C and 30 min at 37°C); 60-min incubation (same as *F*) in the presence of the NOS inhibitor 7-NI (10 μM) (*G*); D-arginine replaced L-arginine in condition *F* (*H*). Data represent the mean ± SD from six independent experiments by using 0.6 mg/ml cardiac SR vesicles. The concentration of SOD was 300 units/ml in all reaction mixtures. ^{45}Ca uptake is inhibited by endogenously produced NO•. The results suggest that cardiac NOS regulates SR ^{45}Ca uptake by directly modifying Ca^{2+}-ATPase function through endogenous NO•.

(Fig. 3 *bD* and *bE*) further demonstrating that cardiac SR NOS is closely related immunologically to the neuronal type NOS. In contrast, no labeling occurred in skeletal muscle SR vesicles (data not shown), suggesting that the localization of nNOS to SR vesicles may be specific to cardiac SR membranes. No immunoreactivity was observed in the absence of anti-nNOS (Fig. 3*bA*) or in the presence of anti-eNOS or anti-iNOS (Fig. 3 *bB* and *bC*). Double immunogold labeling of the vesicles was next used to colocalize cardiac SR NOS with specific SR protein markers in isolated vesicles. Anti-nNOS immunoreactivity colocalized with both SERCA2 and phospholamban antigens (protein markers for cardiac SR, Fig. 3 *bF* and *bH*), but not Na^+,K^+-ATPase (Fig. 3*bG*), a protein marker for sarcolemma membrane), further demonstrating the purity of the isolated SR vesicles and the specificity of the immunogold labeling.

After release of calcium ions from the SR into the cardiomyocyte cytoplasm during muscle contraction, SR Ca^{2+}-ATPase is responsible for active transport of Ca^{2+} back into the SR, triggering relaxation and preparing for the next contraction. To determine whether cardiac SR Ca^{2+}-ATPase is a potential target of NO•, we investigated the effect of endogenously produced NO• on cardiac SR ^{45}Ca uptake under various conditions. Experimental results indicate that endogenously produced NO•, generated by incubation of SR vesicles with NOS substrates and cofactors for 30 min at 37°C, inhibited thapsigargin-sensitive SR ^{45}Ca uptake by 60% (Fig. 4, lane E), and inhibition was over 80% during a 60-min incubation (Fig. 4, lane F). Inhibition of ^{45}Ca uptake was completely prevented in the presence of the NOS selective inhibitor, 7-NI (10 μM, Fig. 4, lane G). To ensure the specificity of endogenous NO• inhibition, SOD (300 units/ml) was added in these experiments, but the amount of SR ^{45}Ca uptake was unaffected (Fig. 4, lane C). When D-arginine replaced L-arginine, no inhibitory effect occurred in the ^{45}Ca uptake as shown in the Fig. 4, lane H. The significant inhibitory effect of NO• on ^{45}Ca uptake suggests that cardiac SR NOS can regulate SR ^{45}Ca uptake by modifying Ca^{2+}-ATPase activity.

DISCUSSION

The studies reported here show immunochemically and biochemically that a neuronal-type NOS is associated with the cardiac SR membrane. The formation of both L-citrulline and NO• radicals from isolated cardiac SR vesicles provide strong evidence that a functional NOS exists on cardiac SR vesicles. Studies have shown that nNOS is located in the endoplasmic reticulum in the rabbit cerebellum (27), but in skeletal muscle, it is restricted to the sarcolemma by a PDZ protein targeting sequence (nNOSμ) (1–4, 7, 28). Our finding that cardiac SR NOS is slightly larger than brain NOS (160 vs. 155 kDa) suggests that cardiac SR NOS may be a new splice or post-translationally modified variant of nNOS. Although cardiac SR NOS migrates at the same molecular mass as nNOSμ, it probably is not an nNOSμ isoform because it was not detected by a specific nNOSμ antibody. Our findings indicate that it is an nNOS isoform as cardiac SR nNOS is readily detected by selective nNOS antibodies and this detection is completely absent in nNOS null mice. Our results show by the immunofluorescence that anti-nNOS immunoreactivity was in a pattern consistent with SR localization in human heart sections, rather than being restricted to the cardiac sarcolemma. Immunogold colocalization studies confirmed nNOS immunoreactivity on cardiac SR vesicles, but not on skeletal muscle SR vesicles, suggesting that the cardiac nNOS isoform may not be the same as that previously described for skeletal muscle (1–4).

It has been reported recently by Zahradnikova *et al.* (10) that eNOS is associated with cardiac SR membrane. However, we could not detect eNOS in our isolated cardiac SR vesicles by either immunogold labeling (Fig. 3) or Western blotting (data not shown). We further tested whether caveola membranes are associated with our SR vesicles because eNOS is targeted to caveolae (29–31). Western blot analysis revealed that caveolae membrane protein, caveolin 3, which is expressed in smooth, skeletal and cardiac muscle, was found in wild-type mice or rabbit whole heart homogenates, but was not detected in our isolated rabbit and mice cardiac SR vesicles or in nNOS knockout-mice cardiac SR vesicles (data not shown). The apparent discrepancy regarding the presence of eNOS on cardiac SR vesicles may possibly be explained by the presence of caveola membranes or sarcolemma in the SR vesicle preparations used in the study by Zahradnikova *et al.* (10). The mechanism underlying the association of nNOS-like NOS with cardiac SR membranes is still unknown. Whether the binding of NOS to cardiac SR is mediated by electrostatic interaction (32–34) remains to be answered.

SR Ca^{2+} stores are central to the dynamic cytosolic Ca^{2+} fluxes that occur during contraction/relaxation cycling in the beating heart. NO• has been found to be an important regulator of muscle contractility (1–8, 25, 26). It has been reported that NO• inhibits both the RyR calcium release channel and force production in skeletal muscle and attenuates cardiac myocyte contraction (35–37). Our results provide new evidence that NO• also can directly down-regulate the SR Ca^{2+}-ATPase and impair the SR calcium transport system (Fig. 4). NO•-induced effects on both the SR Ca^{2+}-ATPase and RyR calcium release channel function (37) could result in a marked alterations in SR Ca^{2+} release, cytosolic Ca^{2+} concentration, and heart muscle contraction. The inhibitory effect of NO• is likely to be further influenced by increases in intracellular calcium as demonstrated previously under ischemic conditions (38). The detailed biochemical mechanism underlying the regulatory effect of NO• on SR Ca^{2+} active transport is not clear. However, NO• may regulate SR Ca^{2+}-ATPase and the RyR by reacting with regulatory thiols of these proteins (39–41) or through a new pathway involving *S*-nitrosoglutathione (42).

The molecular basis for the modulation of heart function by NO• is only partly understood. Our results not only localize a possible new isoform of the neuronal-type NOS on cardiac SR, but also provide evidence for a molecular interaction between NO• and cardiac SR Ca^{2+}-ATPase that may serve to regulate cardiac SR Ca^{2+} active transport. More detailed investigations

of how this NOS isoform is associated with the cardiac SR membrane and how $NO^{\bullet}$ affects SR Ca^{2+} transport in cardiomyocytes, should increase our understanding of the bioregulatory role of $NO^{\bullet}$ in cellular Ca^{2+} homeostasis and cardiac muscle contraction during health and disease.

We are grateful to Dr. Ralph Hruban for providing human heart tissue, Dr. Charles J. Lowenstein for help with the NOS activity assay, and Drs. Peter L. Pedersen, David Proud, Anne Kagey-Sobotka, Periannan Kuppusamy, Jay Zweier, and James Shem for useful suggestions and discussions. We thank Daniel Guastella for maintaining the nNOS knockout colony, Dr. Penghai Wang and Dr. Valerie Roubaud for assistance with the EPR measurements, and Tom Reilly and Michael Delannoy for assistance with confocal microscopy. This work was supported by Grants HL 52175 (to K.Y.X.), HL33360 (to L.C.B.), and P50 HL52315 (to L.C.B., Specialized Center of Research in Ischemic Heart Disease) from the National Heart, Lung and Blood Institute and NS35693 (to D.L.H.), NS33277 (to T.M.D.), and NS34822 (to D.S.B.) from the National Institute of Neurological Disorders and Stroke.

1. Nakane, M., Schmidt, H. H., Pollock, J. S., Forstermann, U. & Murad, F. (1993) *FEBS Lett.* **316,** 175–180.
2. Kobzik, L., Reid, M. B., Bredt, D. S. & Stamler, J. S. (1994) *Nature (London)* **372,** 546–548.
3. Brenman, J. E., Chao, D. S., Xia, H., Aldape, K. & Bredt, D. S. (1995) *Cell* **82,** 743–752.
4. Silvagno, F., Xia, H. & Bredt, D. S. (1996) *J. Biol. Chem.* **271,** 11204–11208.
5. Kelly, R. A., Balligad, J. L. & Smith, T. W. (1996) *Circ. Res.* **79,** 363–380.
6. Michel, T. & Feron, O. (1997) *J. Clin. Invest.* **100,** 2146–2152.
7. Christopherson, K. S. & Bredt, D. S. (1997) *J. Clin. Invest.* **100,** 2424–2429.
8. Campbell, D. L., Stamler, J. S. & Strauss, H. C. (1996) *J. Gen. Physiol.* **108,** 277–293.
9. Xu, L., Eu, J. P., Meissner, G. & Stamler, J. S. (1998) *Science* **279,** 234–237.
10. Zahradnikova, A., Minarovic, I., Venema, R. C. & Meszaros, L. G. (1997) *Cell Calcium* **22,** 447–453.
11. Chu, A., Dixon, M. C., Saito, A., Seiler, S. & Fleischer, S. (1988) *Methods Enzymol.* **157,** 36–46.
12. Xu, K. Y., Zweier, J. L. & Becker, L. C. (1995) *Circ. Res.* **77,** 88–97.
13. Lowry, O. H., Rosebrough, N. J., Farr, A. L. & Randall, R. J. (1951) *J. Biol. Chem.* **193,** 265–275.
14. Bredt, D. S. & Snyder, S. H. (1990) *Proc. Natl. Acad. Sci. USA* **87,** 682–685.
15. Roskams, A. J., Bredt, D. S., Dawson, T. M. & Ronett, G. V. (1994) *Neuron* **13,** 289–299.
16. Xu, K. Y. & Becker, L. C. (1998) *J. Histochem. Cytochem.* **46,** 419–427.
17. Huso, D. L. (1997) *Viral Immunol.* **10,** 15–20.
18. Southan, G. J. & Szabo, C. (1996) *Biochem. Pharmacol.* **51,** 383–394.
19. Handy, R. L., Wallace, P., Gaffen, Z. A., Whitehead, K. J. & Moore, P. K. (1995) *Br. J. Pharmacol.* **116,** 2349–2350.
20. Moore, P. K. & Bland-Ward, P. A. (1996) *Methods Enzymol.* **268,** 393–398.
21. Kuppusamy, P., Wang, P., Samouilov, A. & Zweier, J. L. (1996) *Magn. Reson. Med.* **36,** 212–218.
22. Mayer, B., Klatt, P., Werner, E. R. & Schmidt, K. (1995) *J. Biol. Chem.* **270,** 655–659.
23. Jorgensen, A. O., Shen, A. C., Arnold, W., McPherson, P. S. & Campbell, K. P. (1993) *J. Cell Biol.* **120,** 969–980.
24. Carl, S. L., Felix, K., Caswell, A. H., Brandt, N. R., Ball, W. J., Jr., Vaghy, P. L., Meissner, G. & Ferguson, D. G. (1995) *J. Cell Biol.* **129,** 672–682.
25. Schaart, G., Moens, L., Endert, J. M. & Ramaekers, F. C. (1997) *FEBS Lett.* **403,** 168–172.
26. Kijima, Y., Saito, A., Jetton, T. L., Magnuson, M. A. & Fleischer, S. (1993) *J. Biol. Chem.* **268,** 3499–3506.
27. Hecker, M., Mulsch, A. & Busse, R. J. *Neurochem.* **62,** 1524–1529.
28. Brenman, J. E., Chao, D. S., Gee, S. H., McGee, A. W., Craven, S. E., Santillano, D. R., Wu, Z., Huang, F., Xia, H., Peters, M. F., *et al. Cell* **84,** 757–767.
29. Feron, O., Belhassen, L., Kobzik, L., Smith, T. W., Kelly, R. A. & Michel, T. (1996) *J. Biol. Chem.* **271,** 22810–22814.
30. Garcia-Cardena, G., Oh, P., Liu, J., Schnitzer, J. E. & Sessa, W. C. (1996) *Proc. Natl. Acad. Sci. USA* **93,** 6448–6453.
31. Shaul, P. W., Smart, E. J., Robinson, L., German, Z., Yuhanna, IS., Ying, Y., Anderson, R. G. & Michel, T. (1996) *J. Biol. Chem.* **271,** 6518–6522.
32. Bustamante, E. & Pedersen, P. L. (1980) *Biochemistry* **19,** 4972–4977.
33. Kabir, F. & Wilson, J. E. (1993) *Arch. Biochem. Biophys.* **300,** 641–650.
34. Low, P. S. (1989) in *Red Blood Cell Membranes: Structure, Function, Clinical Implications*, eds. Agre, P. & Parker, J. C. (Dekker, New York), pp. 237–260.
35. Ignarro, L. J. (1996) *Kidney Int. Suppl.* **55,** S2–S5.
36. Brady, A. J., Warren, J. B., Poole-Wilson, P. A., Williams, T. J. & Harding, S. E. (1993) *Am. J. Physiol.* **265,** H176–H182.
37. Meszaros, L. G., Minarovic, I. & Zahradnikova, A. (1996) *FEBS Lett.* **380,** 49–52.
38. Zweier, J. L., Wang, P. & Kuppusamy, P. (1995) *J. Biol. Chem.* **270,** 304–307.
39. Abramson, J. J. & Salama, G. (1989) *J. Bioenerg. Biomembr.* **21,** 283–294.
40. Trimm, J. L., Salama, G. & Abramson, J. J. (1986) *J. Biol. Chem.* **261,** 16092–16096.
41. Stoyanovsky, D., Murphy, T., Anno, P. R., Kim, Y. & Salama, G. (1997) *Cell Calcium* **21,** 19–29.
42. Mayer, B., Pfeiffer, S., Schrammel, A., Koesling, D., Schmidt, K. & Brunner, F. (1998) *J. Biol. Chem.* **273,** 3264–3270.